Ultrasonic Measurement of Weld Penetration

The use of pulse-echo techniques to determine weld pool dimensions is investigated

BY D. E. HARDT AND J. M. KATZ

ABSTRACT. The automatic production of high quality welded joints requires a means of measuring weld quality in real time and a feedback control strategy for regulating that quality. Penetration is a good first order indicator of weld integrity, and most efforts at weld quality control have been concentrated on penetration. In this work, a technique for using ultrasonic pulse-echo measurements to determine weld pool dimensions is examined.

Although current research in nondestructive evaluation indicates that size and shape of discontinuities can be interpreted from the time history of an ultrasonic reflection, the thermal gradients caused by welding cause sufficient distortion in the ultrasound reflection to preclude use of these techniques for initial studies. In a more straightforward approach, a geometric optics framework is developed for the estimation of ultrasonic transit times between an ultrasound transducer and a stationary, hemispherical weld pool in a rod.

Experiments were conducted to verify these predictions by performing measurements of ultrasonic reflections from machined hemispheres and from weld pools in long rods. The results show good agreement between the measurements performed on the cylindrical rods and the geometric optics predictions for both machined surfaces and weld pools.

Introduction

The automatic production of high quality welded joints requires the side-by-side development of techniques for positioning the welding torch (seam tracking) and for regulating welding parameters in real time to obtain a desired level of weld quality. The work described in this paper concentrates on weld penetration as a measure of weld quality using ultrasonic pulse echo techniques to measure the penetration of a weld pool in real time.

Several researchers have considered techniques for measuring weld penetration for feedback control. In 1976, Vroman and Brandt (Ref. 1) used a line scan camera to measure the width of the top side of a weld. Since for a given geometry and fixed welding conditions the depth to width ratio of a weld remains somewhat constant, regulating the top side weld pool width regulates penetration. The results reported were not conclusive and indicated the need for further study of this approach. In a refinement of this technique, Richardson *et al.* (Ref. 2) recently reported the use of video measurement methods to control the topside width of GTA welds. The unique aspect of this work is that the pool is viewed directly from above by putting the optical axis in line with the electrode.

In a more direct approach, Nomura *et al.* (Ref. 3) have used photodetectors placed along the back side of the weldment to measure the back bead width of the weld. As the weld goes from partial to full penetration, the infrared radiation from the back side of the weld goes through a step transition. In this way, photodetectors can be used to detect a full penetration weld. Garlow (Ref. 4) and Reiff (Ref. 5) have used a simple phototransistor to measure the back side weld bead width in GTA welds with reasonable accuracy. This measurement was used in a closed loop controller that quite accurately regulated the back bead width. However, back side weld bead sensing has an inherent drawback in that it is difficult or impossible to conveniently locate a sensor on the back side of the weldment for many weldment configurations. In addition, back side sensing does not provide useful measurements when knowledge of partial penetration is desired.

Hardt and Zacksenhouse (Ref. 6) demonstrated that weld pool size could be determined by measuring the resonant frequency of a full penetration pool. The pool is modelled as a dynamic mass spring system, and they show that the natural frequency of this system is a function of the size of the weld pool. The existence of this frequency dependence on weld pool size has been verified experimentally, and the present work is attempting to show that arc voltage frequency measurements can be used to determine the weld pool natural frequency. Renwick and Richardson (Ref. 7) have also observed a pool resonance in the case of a partially penetrated weld.

All of the weld pool measurement techniques mentioned so far share the difficulty that they are attempting to measure variables that are not single valued indicators of penetration. In an attempt to provide a means of directly measuring the desired weld pool dimensions, the concept of using ultrasonic pulse echo techniques to directly measure weld pool dimensions was developed, based upon established technology for other applications. In this paper, the techniques available for ultrasonic measurement and the implications of application to in-process welding are discussed. This is followed by a critical experiment where the existence of reflections from a weld pool are confirmed, and some rudimentary depth measurements performed.

Ultrasonic Methods for Defect Measurement

Ultrasonic testing has been used effectively as a nondestructive evaluation

D. E. HARDT and J. M. KATZ are with the Laboratory for Manufacturing and Productivity, Massachusetts Institute of Technology, Cambridge, Massachusetts.

Sept. 1984

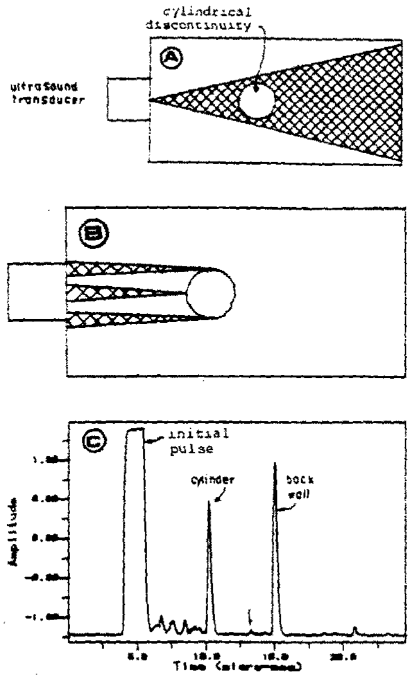

Fig. 1 – Ultrasonic reflections from a cylindrical discontinuity (Ref. 11): A – ultrasound incident upon cylindrical discontinuity; B – ultrasonic reflections from a cylinder; C – oscilloscope trace of reflections from cylinder

technique for locating discontinuities below the surface of various metals. It has become a standard technique for locating cracks, lack of fusion, porosity, and other discontinuities in fusion welds. All ultrasonic testing methods are based on reflection of stress waves caused by changes in the material properties of the medium in which it travels. This makes single point range measurements a simple matter of measuring the transit time for a single ultrasound pulse to travel to and from a reflector. However, a discontinuity of dimension larger than the wavelength of the incident ultrasound pulse will not only reflect ultrasound, but it will rearrange the phase relationship of the incident ultrasound pulse. Thus, the "shape" of the reflected ultrasound pulse is different from the "shape" of the incident pulse – see Fig. 1 and Freeman (Ref. 8). The manner in which the pulse "shape" is altered is a function of the size, shape, and material properties of the reflector. Thus the reflected ultrasound pulse contains information concerning the size and shape of whatever caused the reflection.

Many nondestructive testing problems require knowledge of discontinuity size and/or shape as well as the location of a discontinuity, and several researchers have been studying ultrasonic techniques for directly determining the size and shape of the defects in materials. These techniques generally involve some deciphering of the characteristics of ultrasonic reflections from idealized defects like spheres, cylinders and disks. These studies include both time domain (Pao and (Ref. 9) and frequency domain (Ref. 10)) approaches and include techniques that determine size from a single reflection (Ref. 11) or by observing the scattered intensity at several different locations (Refs. 12, 13).

The results of these studies indicate that the ultrasonic reflections from a given "target" are a function of both size and shape of the reflector. If the essential features of ultrasonic reflections from known surfaces can be characterized, it should be possible to develop a means of measuring reflector dimensions from ultrasound traces. Sachse (Ref. 11) has done this for the case of a fluid filled cylindrical inclusion in an aluminum block while Thompson and Thompson (Ref. 14) have performed studies using a frequency domain scattering technique for identifying a more general target. In yet another approach, Rose (Ref. 15) has used computer pattern recognition techniques to identify certain postweld discontinuities in welded steel plates.

Ultrasonic Measurement of Weld Pool Dimensions

A weld pool constitutes a change in phase and material properties relative to the rest of the weldment and thus should be a reflector of ultrasound. Tabulated values of the density and speed of sound of molten aluminum and copper (Ref. 16) indicate that a weld pool in either of these materials would indeed reflect ultrasound. Since the wavelength of ultrasound is smaller than the characteristic dimension of any but the thinnest of materials that one might wish to weld, an ultrasound pulse reflected by a weld pool should contain information concerning the size of that weld pool.

In this paper the conditions for reflecting ultrasonic waves from a weld pool are examined, and a means for interpreting such reflections is presented. A critical experiment is performed to demonstrate the ability of ultrasound to measure the depth of penetration of a static weld pool. There are, however, several areas of research that must precede the development of an ultrasonic weld pool measurement system. The bulk of these are the result of the large temperature gradients that exist within a weldment.

The propagation speed of ultrasound is a function of the temperature of the medium in which it travels. In general, this speed drops as the temperature of the medium increases. For weld pool measurement, this will result in an ultrasound velocity that varies with position. This velocity gradient can cause shifting of the path followed by an ultrasound pulse and may make it difficult to "see" reflections from the weld pool.

High temperatures also cause an increase in attenuation of the medium. Thus larger amplitude ultrasound pulses must be applied to the medium in order to get a measurable reflection back. In the heat-affected zone (HAZ) of the weld, the solid phase transition can result in a large enough variation in properties to cause reflections of ultrasound (Ref. 17). If the magnitude of this reflection is large, it may not be possible to transmit ultrasound through the HAZ to the weld pool. This would limit the ultrasonic technique to one of measuring the dimensions of the HAZ. On the other hand, if finite but small reflections from the HAZ exist, it might be possible to independently measure the size of the HAZ and of the weld pool. This would present the opportunity for independent control of HAZ dimensions and the penetration.

Another problem is that an ultrasound transducer must be in acoustic contact with the material to be inspected if any energy transfer is to take place. This is normally accomplished by using a liquid or gel to fill in the asperites between the transducer and the object to be inspected or by clamping the transducer to the specimen with a large force (Ref. 18). A weld pool measurement system such as that shown in Fig. 2 must be capable of moving along the top surface of a hot weldment while maintaining

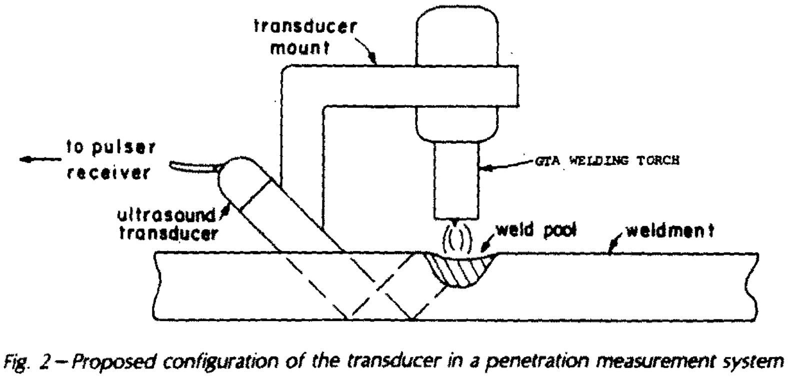

Fig. 2 – Proposed configuration of the transducer in a penetration measurement system

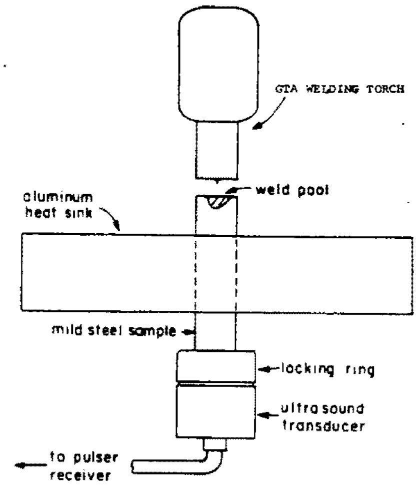

Fig. 3 – Configuration for detecting ultrasonic reflections from a weld pool

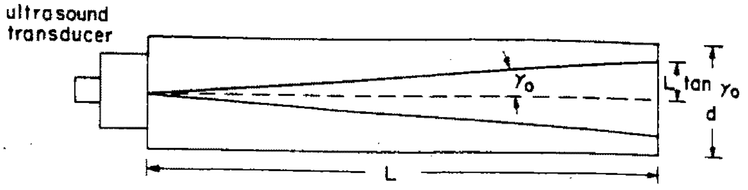

Fig. 4 – Transmission of ultrasound through a flat ended rod

acoustic contact between the transducer and the weldment.

Currently, four approaches to the problem have been considered. The first technique consists of a standard contact angle beam transducer that is lightly held against the weldment by a spring force so that it is still free to slide over the weldment. The second technique would employ a commercially available wheel shaped transducer that is filled with water. The third technique would employ a linear actuator to lift the transducer off of the weldment, discretely advance the weld torch, and then compress the transducer back down on the weldment (Ref. 19). The fourth and by far the most elegant technique would be to employ an electromagnetic acoustic transducer (EMAT), see Thompson and Thompson (Ref. 14), as the ultrasound source. EMAT's provide a non-contact method of performing ultrasonic inspection that is clearly desirable for the case of weld pool dimension measurement. Unfortunately, state-of-the-art EMAT's have low transduction efficiencies.

Weld Pool Reflections in a Cylindrical Rod

In order to measure the dimensions of a weld pool using ultrasound, it is necessary to determine how the presence of a weld pool reflects an ultrasound pulse and then how the dimensions of the reflecting weld pool can be isolated from a time trace of the ultrasound pulse. To this end, a simplified weldment geometry (a cylindrical rod) combined with a ray optics wave analysis was employed. (The results of Schmitz (Ref. 20) are encouraging with regard to the utility of this approach.)

The case of ultrasonic weld pool dimensional measurement lends itself to the geometric optics approach, since the location of the weld pool is known. By physically connecting the transducer mounting structure to the welding torch, it can be guaranteed that the transducer will track the weld pool at all times. Using the ray tracing techniques of geometric optics, it is possible to reconstruct a surface profile of the weld pool from ultrasonic time traces. Important concepts for such a reconstruction are discussed below.

Consider the configuration shown in Fig. 3 where an ultrasound transducer is clamped to the end of a cylindrical rod. A GTA welding torch is placed above the rod end opposite to the transducer, and a weld pool is established in the rod end. In this configuration, the ultrasound transducer will be directly viewing the weld pool as it forms. However, before considering the reflections of ultrasound from a weld pool, it is well to look at the ultrasonic reflections from the end of a plain cylindrical rod of length L, and diameter d.

In Fig. 4, an ultrasound transducer with maximum beam angle is shown placed on the end of the rod (positioned such that its center is aligned with the rod axis and that the geometry is axially symmetric). This will allow the use of a two dimensional model of the ultrasonic ray paths. In order to simplify the discussion, it is assumed that $L(\tan(\gamma))$ is less than half the rod diameter so that the ultrasound pulse will reach the opposite rod end before the beam spreads out enough to reach the sidewalls of the rod.

The ultrasound beam can be described by a series of rays traveling down the length of the rod. The rays will make an angle θ with the axis of the rod such that θ is less than the absolute value of the transducer beam angle. For an arbitrary ray with angle θ, the time required for ultrasound to travel from the transducer to the opposite rod end is given by: $t_1 = L/c_1 \cos(\theta)$ where c_1 is the longitudinal wave speed.

The rod end is a boundary between a solid and air so refraction from the rod end will not take place. From Snell's law it can be shown that the longitudinal pulse is reflected at the same angle as the incident pulse while the reflected shear pulse has an angle given by: $\theta_{rt} = \sin (c_t/c_1 \sin \theta)$ where c_t is the shear wave speed. The radial position at the rod end is given by:

$$r = L \tan \theta \tag{1}$$

It is possible for ultrasound to return to the transducer along several different paths, and Fig. 5 depicts four possible

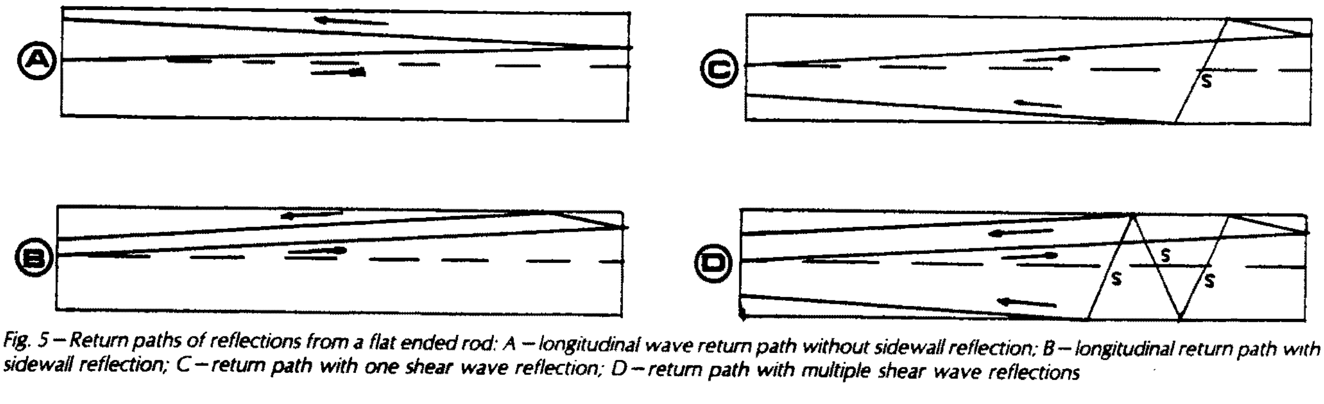

Fig. 5 – Return paths of reflections from a flat ended rod: A – longitudinal wave return path without sidewall reflection; B – longitudinal return path with sidewall reflection; C – return path with one shear wave reflection; D – return path with multiple shear wave reflections

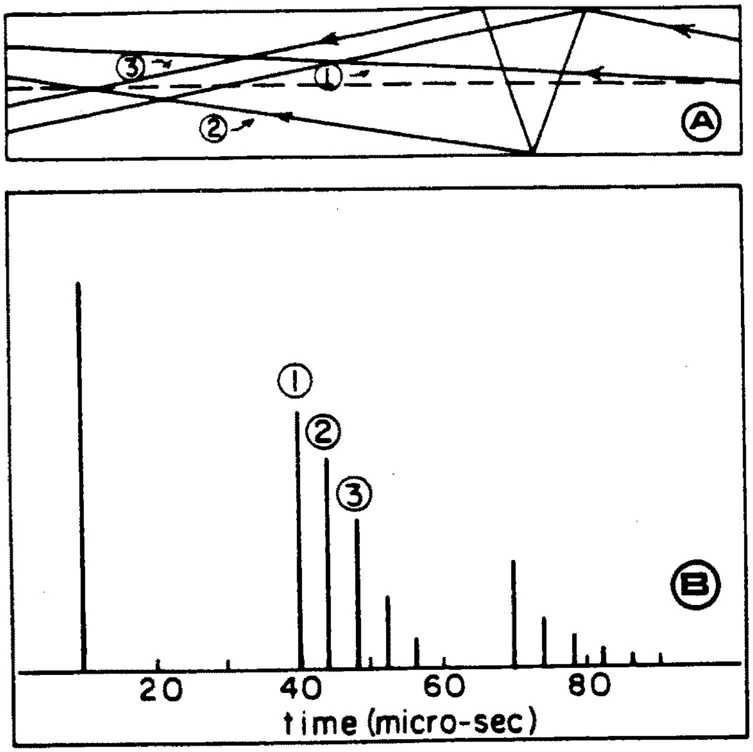

Fig. 6 – Reconstruction of ultrasound reflections in a cylindrical rod: A – some possible ray return paths; B – reconstructed waveform (3½ in. long rod)

paths. Since the beam angle is such that the ultrasound reaches the far end of the rod before the side walls, all of the paths have a transit time of:

$$t = L/c_1 \cos \Theta \qquad (2)$$

to the far end of the rod. The return path can consist of a longitudinal pulse or can be mode converted to [up to n] shear pulse reflections, where n is given by:

$$n < \frac{(4\,L \tan\Theta\, d)\ 1-(c_t/c_1)^2 \sin^2\Theta}{2\,d\,(c_t/c_1)\sin\Theta\tan\Theta} \qquad (3)$$

This condition ensures that the distance travelled as shear waves does not exceed the length of the rod.

Under these conditions, the transit time for an ultrasonic pulse to travel from the transducer to the rod end and back with up to n shear pulse reflections is:

$$t = \frac{2\,L}{c_1 \cos\Theta} + \frac{(c_1^2 - c_t^2)\qquad nd}{c_1\,c_t\ \ (c_1^2 - c_t^2)\cos^2\Theta} \qquad (4)$$

The first term in equation (4) is the time required for a longitudinal pulse to travel down the rod and back. The second term is the additional return time required for n shear pulse reflections along the side walls of the rod. (Note that shear pulses are slower than longitudinal pulses.)

For most real transducers, γ and hence Θ are small so equation (4) can be simplified using a small angle approximation to find the transit times:

$$t = \frac{2L}{c_1} + \frac{nd\sqrt{c_1^2 - c_t^2}}{c_1 c_t}. \qquad (5)$$

Thus we expect the time traces of ultrasonic reflections from the end of a cylindrical rod to consist of a peak at $t = 2L/c_1$ and a train of trailing peaks delayed from the first peak by the term:

$$t = \frac{d\sqrt{c_1^2 - c_t^2}}{c_1 c_t} \qquad (6)$$

Figure 6 is a reconstruction of such a time trace. The amplitudes of the returning pulses are a function of the amplitude distribution of the transducer and are inversely proportional to the length of the ray path. Thus we expect to see the pulses occurring at later times diminished in amplitude. This effect is shown in Fig. 6. Because there is a dependence on angle in the transit time equations, it is expected that the distinct peaks of Fig. 6 will be spread out in a real ultrasonic time trace. Finally, the energy returning to the transducer end of the rod can reflect from the rod end and travel down and back again. This will result in a duplication of the ultrasound time trace just described but delayed in time by $2L/c_1$.

The above discussion indicated that ultrasonic reflections in a cylindrical rod have a complicated structure resulting from the geometry of the rod and the existence of mode conversion between longitudinal and shear pulses. This is also true in the case of ultrasound transmission in a plate, which more accurately describes a general weldment configuration.

Reflections from a Weld Pool on the End of a Cylindrical Rod

If we assume that the shape of a stationary weld in a thick weldment can be approximated as a hemisphere, we can consider a hemispherical shaped weld pool of radius r at the end of a cylindrical rod of length L, as in Fig. 7. Since the rod is axially symmetric, the weld pool can be described as a 2-dimensional surface:

$$(L - x)^2 + r^2 = r_p^2 \qquad (7a)$$

and,

$$\frac{dr}{dx} = \frac{L - x}{(r_p^2 + 2Lx - (x^2 + L^2))^{1/2}} \qquad (7b)$$

where 2r is less than the rod diameter, d.

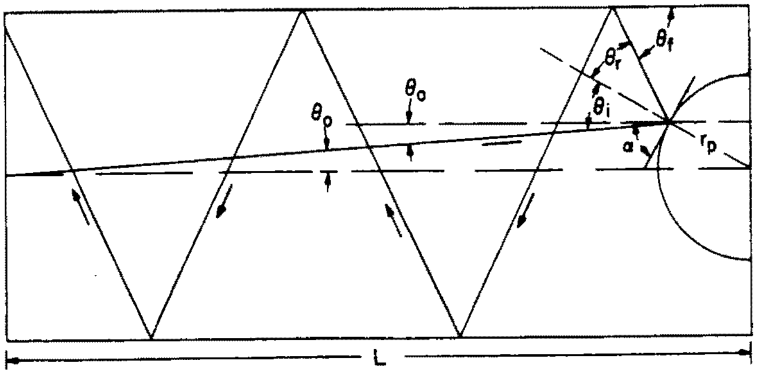

Fig. 7 – Reconstruction of ultrasound reflections in a cylindrical rod

If we assume that an ultrasound ray with angle θ to the rod axis is incident upon the weld pool, an arbitrary point on the ray path can be described by the equation:

$$r = x \tan \theta. \qquad (8)$$

The point of intersection between the ray path and the weld pool (x_i, r_i) can be found by solving equations (7a) and (8) simultaneously with the result:

$$x_i = L \cos^2\theta - L \cos \theta \, (r_p^2/L - \sin^2 \theta)^{1/2}$$

and,

$$r_i = 0.5L \sin 2\theta + L \sin \theta \, (r_p^2/L^2 - \sin^2 \theta)^{1/2}$$

$$(9)$$

The angle of incidence of the incoming ultrasound ray is a function of θ, and the tangent angle of the weld pool surface (Fig. 7) and is given by:

$$\theta_i = 90 \text{ deg} + \theta - \alpha$$

In turn, the tangent angle α is related to the slope of the weld pool surface by:

$$\alpha_i = \tan^{-1} dr_i/dx_i$$

$$= \tan^{-1} \frac{L - x}{r_p^2 + 2Lx - (x^2 + L^2)} \qquad (10)$$

The angle of reflection from the weld pool can be found using Snell's law again with $\theta_r = \theta_i$ for longitudinal reflections and equation (9) for shear reflections. For convenience, the reflection angle can be expressed as an angle relative to the rod axis, θ (Fig. 7) using:

$$\theta_f = \theta_i - \theta + \theta_r \qquad (11)$$

There are 4 basic return paths back to the transducer from the weld pool. These return paths and their respective transit time equations are listed below; the return paths are also depicted in Fig. 8.

1. Longitudinal reflection with direct return to transducer:

$$t = \frac{x_i}{c_1 \cos \theta} + \frac{x_i}{c_1 \cos \theta} \qquad (12a)$$

2. Longitudinal reflection which then reflects from a sidewall, goes through n-shear wave reflections, and then returns as a longitudinal pulse:

$$t = \left[\frac{1}{\cos \theta} + \frac{1}{\cos \theta_f} \right] \frac{x_i}{c_1} + \qquad (12b)$$

$$\left[\frac{c_1^2 - c_t^2}{c_1 c_t} \right] \frac{nd}{(c_1^2 - c_t^2 \cos^2\theta)^{1/2}} \cdot$$

where: $n <$

$$\frac{[x_i (\tan \theta_f + \tan \theta) - d/2] \; (c_1^2 - c_t^2 \cos^2 \theta)^{1/2}}{d c_t \cos \theta_f}$$

(Note that the equations for reflections from a flat ended rod are a special case of this equation.)

3. Shear reflection which returns directly to transducer:

$$t = \left[\frac{1}{c_1 \cos \theta} + \frac{1}{c_t \cos \theta_f} \right] x_i \qquad (12c)$$

4. Shear wave reflection which is mode converted back to longitudinal wave after n reflections:

$$t = \left[\frac{1}{c_1 \cos \theta} + \frac{c_t}{c_1^2 \cos \theta_f} \qquad (12d)\right.$$

$$\left. \left[\frac{c_1^2 - c_t^2}{c_1 c_t} \right] \frac{\tan \theta}{\sin \theta} \right] x_i +$$

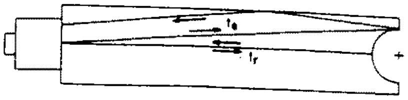

Fig. 9 – Comparison between the path length to weld pool bottom and rod end

$$\left[\frac{c_1^2 - c_t^2}{c_1 c_t} \right] \frac{(2n + 1)d}{2 \sin \theta_f}$$

where: $n < [\tan \theta_f + \tan \theta] \frac{x_i}{d} - \left(\frac{1}{2} \right)$

The relationships between the different transit times are very much a function of the radius of the weld pool and the length of the rod which serve to determine the coordinates of the reflection point (x_i, r_i), and the angle of reflection. The amplitudes of the reflected pulses are also functions of the angles of incidence and the path lengths. The shape of the final ultrasound time traces thus varies with the radius of the weld pool. It is clear from the equations that there will be some type of multiple peak structure as in the case of the flat ended rod. This is a result of the difference in speed of sound between longitudinal and shear waves and the difference in path length between the various possible paths.

If ultrasonic reflections from a weld pool are used to determine the dimensions of the weld pool, it will be necessary to isolate characteristics of the ultrasonic time traces to allow one to determine those dimensions. Equation (12) is somewhat cumbersome for this purpose. However, a simplification provides an estimate of the radius of a hemisphere shaped weld pool in the end of a rod.

Consider a "small" hemisphere on a rod end such that the incident ultrasound beam will be reflected from part of the flat portion of the rod end as in Fig. 9. This will result in a reflection from the rod end which should be a dominant characteristic of the ultrasound time trace. The

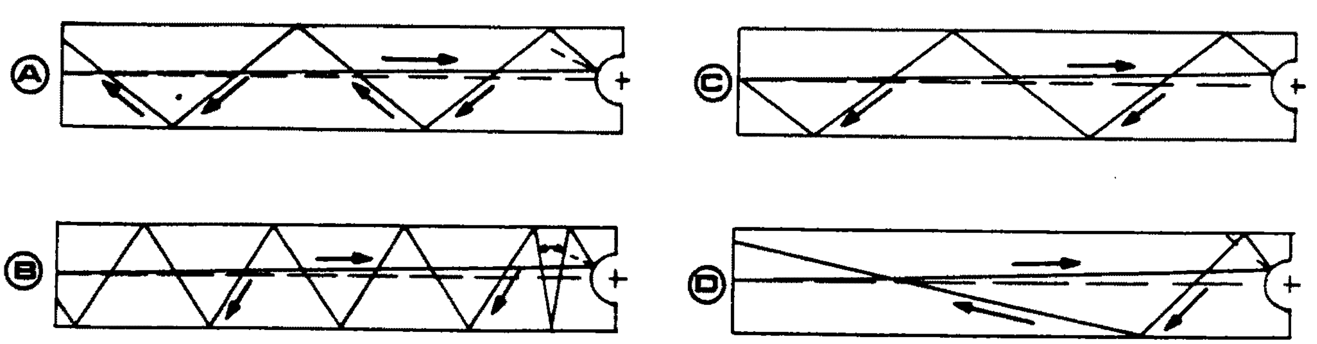

Fig. 8 – Ultrasonic reflections from a hemisphere shaped weld pool in a cylindrical rod: A – longitudinal return path; B – longitudinal reflection mode converted to shear and then back to longitudinal; C – shear return path; shear reflection mode converted to longitudinal

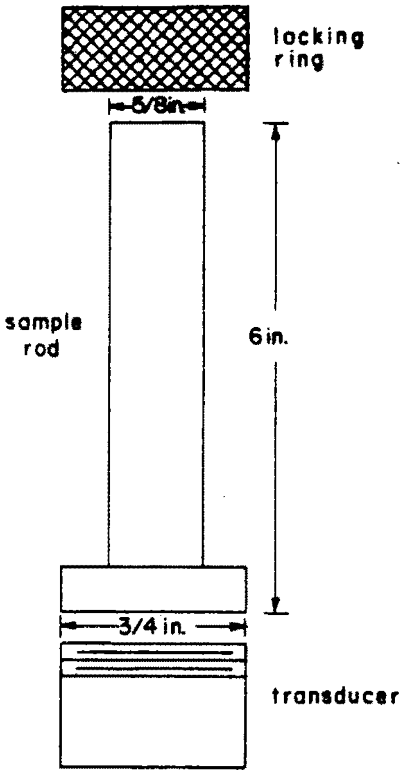

Fig. 10 – A cylindrical rod sample showing the transducer mount and clamping ring

shortest transit time to the flat portion of the rod end is given by:

$$t_e = \frac{2\,(L^2 + r_p^2)^{1/2}}{c_1}$$

However, the first ultrasound reflection that returns to the transducer in this case follows a path down the center of the rod at 0 = 0 to the bottom of the weld pool and back. This path will have a transit time given by:

$$t_e = \frac{2(L - r_p)}{c_1}.$$

If the ultrasound peaks corresponding to these two transit times could be isolated and their difference, Δt, measured, the radius of the weld pool could be determined as follows:

$$\Delta t = t_e - t_r$$

$$= 1/c_1\,[L^2 + r_p^2 - 2(L - r_p)]$$

which can be solved for r_p, yielding:

$$r_p = \frac{Lc_1\Delta t + c_1^2\,t^2/4}{2L + c_1\Delta t}. \qquad (13)$$

The validity of this expression has been evaluated experimentally and is discussed below.

Cylindrical Rod Experiments

The cylindrical geometry analyzed above was used in a series of experiments with the objectives of:

1. Establishing whether ultrasound is indeed reflected from weld pools.
2. Establishing the validity of equation (13).

To separate the effect of temperature gradients on this result, two different experiments were performed. In the first, hemispheres of various radii were machined into the rod and then the radius was measured from the ultrasound reflections and equation (13). In the second set of tests, a GTA torch was used to create various size weld pools on the flat end of a rod. Ultrasound measurements were again made and the depth of the weld pool estimated by application of equation (13).

The test pieces were turned from 1020 hot rolled steel to a diameter of 15.8 mm (5/8 in.) and a length of 152.4 mm (6 in.). The weld pool experiments were performed using a DC welding power sup-

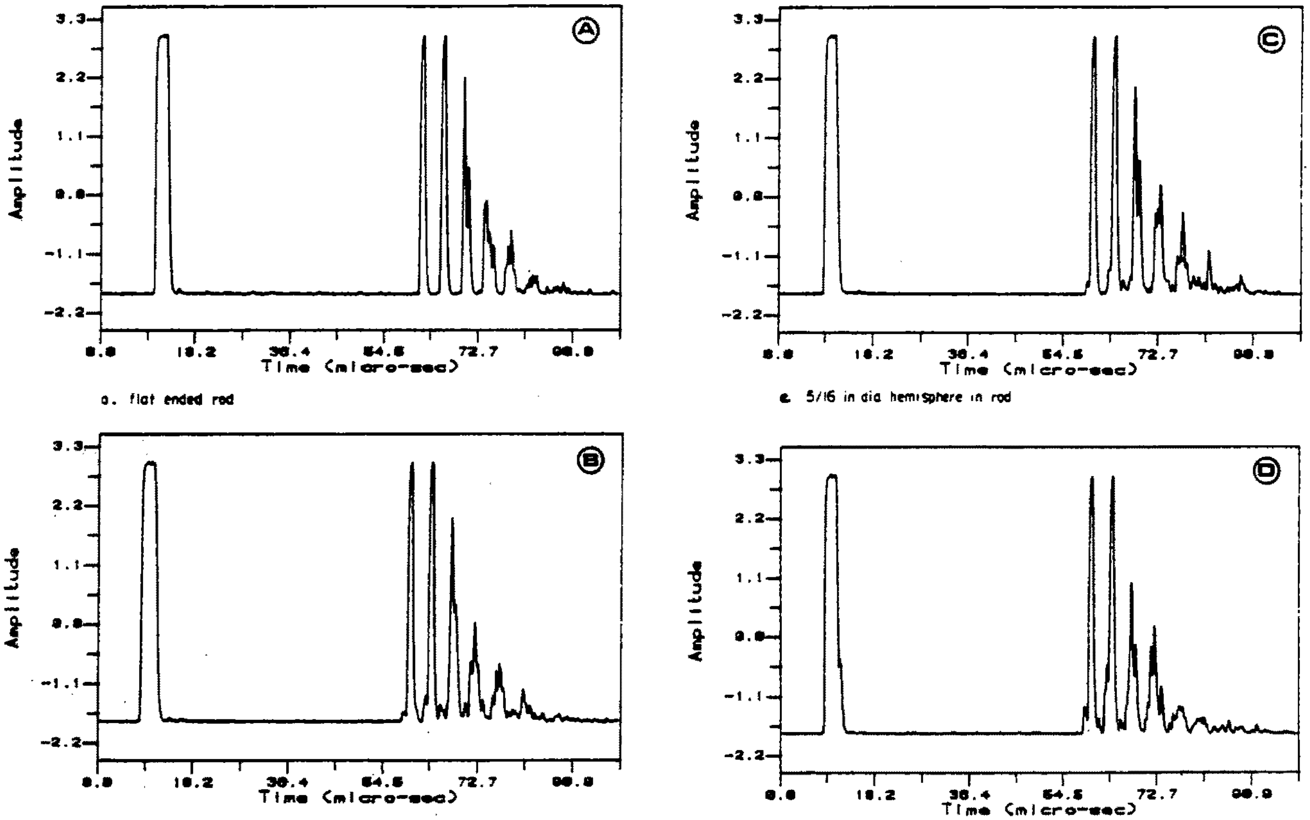

a. flat ended rod

c. 5/16 in dia hemisphere in rod

b. 3/16 in. dia. 1/4 in. deep hemisphere in rod

d. 3/8 in. dia. hemisphere in rod

Fig. 11 – Recorded reflections from hemispheres of various radius rods: A – flat ended; B – 3/16 in. diameter, 1/4 in. deep hemisphere; C – 5/16 in. diameter hemisphere; D – 3/8 in. diameter hemisphere

ply connected to an air-cooled GTAW torch with a 3.2 mm (⅛ in.) 1% thoria tungsten electrode. Argon shielding gas was used for all of the experiments.

A Krautkramer USM-2 ultrasonic pulser-receiver unit was used as the ultrasound source. The transducer was a Panametrics A611S, 10 MHz, 12.7 mm (½ in.) diameter delay line transducer. The A611S is threaded so that a delay line can be connected to the transducer using a locking ring to hold it down, as depicted in Fig. 10. The transit time of ultrasound through the rod is expected to be of the order of 50 micro-sec. To extract weld pool dimensional information from the signals, time resolution of the order of 0.1 micro-seconds(s) is necessary.

To record and display the ultrasound reflections, a system comprising a Tektronix 7854 digital oscilloscope coupled to a DEC MINC lab computer was employed. By allowing communication between these devices on an IEEE General Purpose Interface Bus (GPIB), the high speed digitizing and signal averaging capabilities of the oscilloscope could be exploited. At the same time, the MINC was used to control the functions of the oscilloscope during the experiment, record the data on disk, and plot the resulting waveforms. Since the 7854 has a bandwidth >100 MHz, recording ultrasonic reflections was well within its capabilities.

The first set of measurements were performed on 8 rods: 1 flat ended rod, and 7 with hemispheres of diameter between 4.76 mm (3/16 in.) and 12.7 mm (½ in.) ball end milled into the rod end. Typical results are shown in Fig. 11.

Figure 11A depicts the ultrasonic reflections from a flat ended rod. Here the transit time from the initial pulse to the first reflected pulse is 51.56 micro-s. From equation (1), this is equivalent to a rod length of 152.1 mm (5.98 in.).

The spacing between the trailing peaks is 4.17 micro-s. Equation (6) was developed to predict the spacing between these peaks. Rearranging this expression to estimate rod diameter from the peak spacing, we find that d = 16.01 mm (0.63 in.). The estimates of rod length and diameter from equations (1) and (6) are in good agreement with the actual values of length (152.4 mm or 6 in.) and diameter (15.86 mm or 0.62 in.).

Typical time traces of ultrasonic reflections from hemispherical ball end milled surfaces are contained in Figs. 11B and D. These samples were manufactured using ball end milling cutters ranging in diameter from 4.76 mm (3/16 in.) to 12.7 mm (½ in.) in increments of 1.59 mm (1/16 in.). Examining the data sequentially, the first thing to notice is that a shoulder forms on the first reflection and breaks off into a second peak as the hemisphere becomes larger. This first small peak is postulated to be a reflection from the bottom of the hemispherical surface as depicted in Fig. 9.

The next feature to notice is the smearing out of the reflection as the size of the reflector increases. Figure 11A shows a set of very clearly defined peaks. As one goes through to Fig. 11D, there are more and more reflections between the large peaks. These are the result of reflections from different portions of the curved surface which result in an almost continuous variation in transit time. Intermediate peaks exist between the major peaks found in the flat ended rod. These are probably results of the hemisphere reflections being mode converted to shear waves in the rod.

In an attempt to measure the dimensions of these hemispheres, the time difference between the small initial peak or shoulder and the first major peak of the ultrasound time traces was measured. The rods were then sectioned down the middle and the depths of each of the hemispheres was measured using a Nikon toolmaker's microscope. Figure 12 is a plot of the measured time difference vs. the depth of the hemisphere. Also shown in Fig. 12 is the theoretical relationship between the time difference between the first two peaks of an ultrasonic time record and the hemisphere radius according to equation (13) and using the simplest approximation:

$$\Delta t = 2c_1 r_p \tag{14}$$

There is reasonable agreement between theory and the measurements. It appears that either of these approximations could be used to give a first order estimate of the relationship between hemisphere size and the spacing of the first two reflected peaks.

After completing the studies with the milled hemispherical surfaces, a set of experiments were performed producing weld pools on the end of some of the sample rods and obtaining ultrasonic reflections using the MINC-7854 data acquisition system. Figures 13A and D are ultrasonic time traces obtained while welding the ends of four of these sample rods.

The first noticeable feature in these traces is the large amount of noise present between the initial pulse and the first returned reflection as noted in Fig. 13A. This noise does not appear in the traces between pulses and appears to attenuate with time. This seems to indicate that the noise is in fact caused by reflections from something present in the rod. This could be the result of material variations or inclusions of oxide or carbon present in the rod. At low temperatures the material properties of such inclusions may not vary enough from the properties of steel to cause reflections. However, the material properties of these inclusions at elevated temperatures can be different from those of steel resulting in reflections from the inclusions.

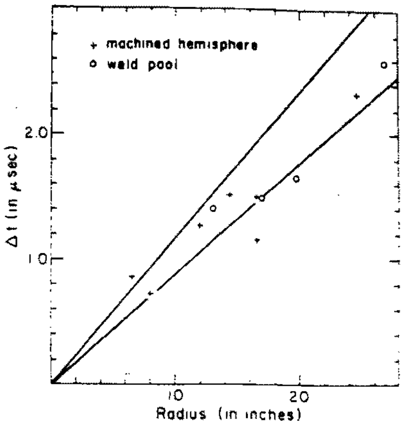

Fig. 12 — Shoulder-to-peak time difference vs. hemisphere and pool radius. The lower line represents the prediction of equation (14) while the upper is from equation (13)

The amplitudes of the rod end reflections in Figs. 13A and D are much smaller than those in Figs. 11A and D. This is a result of the increased attenuation as the rod heats up. The transit times to the first rod end reflection are on the order of 53 micro-s, roughly 2 micro-s slower than in the case of the cold rods. This corresponds to an average speed of sound in the rod of 5750 m/s as opposed to the speed of sound in a rod at room temperature which is 5900 m/s. Finally, notice the presence of multiple pulses in the rod end reflections. These resemble the reflections from rods with milled hemispheres, although attenuated in amplitude.

The time difference between the small, initial peak and the first major peak was again measured, and equation (13) was applied to estimate the pool depth. (Although identifying this initial peak appears tenuous from Fig. 13, it was easily and consistently distinguished from noise by examination of the digitally stored ultrasound signal.) After welding, the rods were sectioned and etched with a Nital solution and the weld pool dimensions measured using the toolmaker's microscope. These measurements have been plotted against the corresponding time difference between the first two reflection peaks in Fig. 12. These results clearly fall along the theoretical curve to first order. While there are not many data points, it seems clear that the ultrasonic reflections from the region of a weld

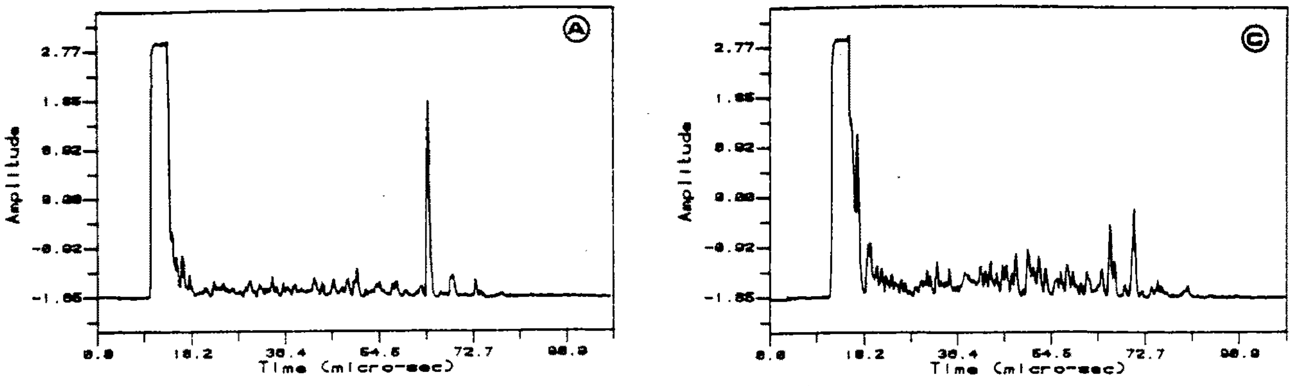

a. .13 in. deep

c. .19 in. deep

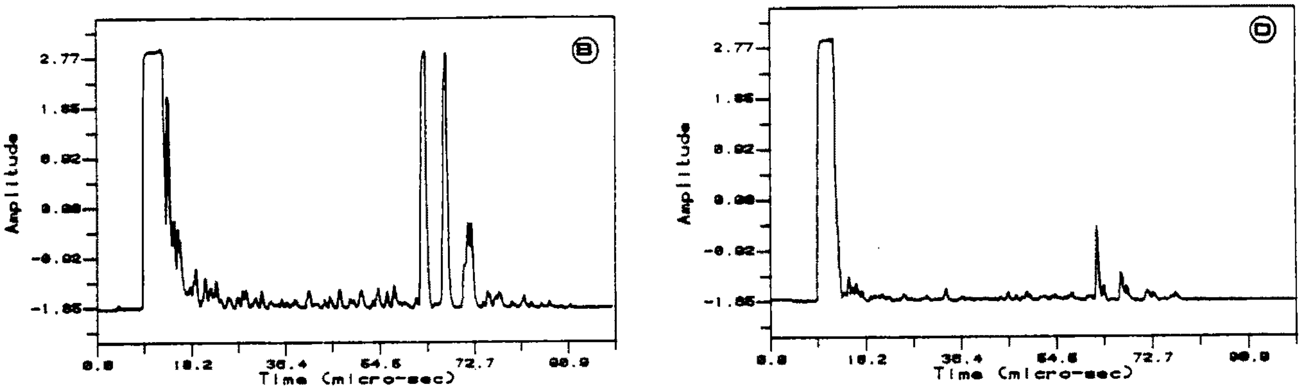

b. .17 in. deep

d. .27 in. deep

Fig. 13 — Reflections from weld pools of various depths: A — 0.13 in. deep; B — 0.17 in. deep; C — 0.19 in. deep; D — 0.27 in. deep

pool are behaving as expected.

Conclusion

The concept of using reflection ultrasound methods to measure the size of a weld pool in-process has been advanced. While techniques for direct shape measurement by decoding the entire ultrasound reflection are under development, the additional problems introduced by high temperatures and large temperature gradient in welding requires that simpler approaches be first considered.

In this paper, the reflection pattern from hemispheres in the end of long cylinders have been predicted and verified experimentally. More importantly, when the hemispherical shape represents the weld pool-solid metal interface, it has been shown that accurate radius measurements can be made. Since the completion of this work, results of a similar concurrent study by Lott (Ref. 21) have been reported, with similar conclusions regarding weld pool size measurement. Thus the initial step toward realization of real time weld pool cross section measurement for in-process control purposes has been successful.

Acknowledgments

The work discussed in this paper was supported by the U.S. Office of Naval Research under contract no. N00014-80-C-0384.

References

1. Vroman, A. R., and Brandt, H. 1976. Feedback control of GTA welding using puddle width measurements. *Welding Journal* 55(9): 742-749.

2. Richardson, R. W., Gutow, D. A., and Rao, S. H. 1982 (Nov.). A vision based system for weld pool size control. *Measurement and control for batch manufacturing,* ASME Special Publication. pp. 65-75.

3. Nomura, *et al.* 1980 (Sept.). Arc light intensity controls current in SA welding system. *Welding and Metal Fabrication:* 457-463.

4. Garlow, David. 1982 (June). *Closed loop control of full penetration welds using optical sensing of back bead width.* S.M. Thesis, Dept. of M.E., MIT.

5. Reiff, J. R. 1983 (Feb.). *Closed-loop control of backside puddle width in the gas tungsten arc weld process.* M.S. thesis, Department of Mechanical Engineering, M.I.T.

6. Zacksenhouse, M., and Hardt, D. E. 1983 (Oct.). Weld pool impedance identification for size measurement and control. *Trans. ASME, Journal of Dynamic Systems, Measurement and Control* 104 (3).

7. Richardson, R. W., and Renwick, R. J. Experimental investigation of GTA weld pool oscillations. *Welding Journal* 62(2):29-s to 35-s.

8. Freeman, A. 1962. A mechanism of acoustic echo formation. *Acoustica* 12. 10-21.

9. Pao, Y. H. and Wolfgang Sachse. 1974 (Nov.). Interpretation of time records and power spectra of scattered ultrasonic pulses in solids. *J.A.S.A.* 56(5): 1478-1486.

10. Gericke, D. R. 1963. Determination of the geometry of hidden defects by ultrasonic pulse analysis testing. *J.A.S.A.* 35: 364.

11. Sachse, Wolfgang. 1975 (April). Determination of the size and mechanical properties of a cylindrical fluid inclusion in an elastic solid. *Materials Evaluation* 33: 81-88.

12. Tittman, B. R. *et al.* 1978. Scattering of longitudinal waves incident on a spherical cavity in a solid. *J.A.S.A.* 63(1): 68.

13. White, R. M. 1958. Elastic wave scattering at a cylindrical discontinuity in a solid. *J.A.S.A.* 30(8): 771-785.

14. Thompson, D. O. and Thompson, R. B. 1979. Quantitative ultrasonics. *Phil. Trans. R. Soc. London.* 292: 233-250.

15. Rose, J. L. *et al.* 1980 (Aug.). Flaw classification in welded plates using a microprocessor controlled flaw detector. *NDT Inter-*

national 13(4): 159-164.

16. Webber, G. M. B., and Stephens, R. W. B. 1968. Transmission of sound in molten metals. *Physical acoustics: principles and methods*, ed. by Warren P. Mason. New York: Academic Press.

17. Papadakis, E. P. *et al.* 1972. Ultrasonic attenuation and velocity in hot specimens by the momentary contact method with pressure coupling and some results in steel to 1200 C. *J.A.S.A.* 52(3): 850-857.

18. Carnevale, E. H. *et al.* 1964. Ultrasonic evaluation of elastic moduli at elevated temperatures using momentary contact. *J.A.S.A.* 36(9): 1678-1684.

19. Rumbold, J. G. and Krupski, S. 1981. Ultrasonic thickness variation measurement of hot forged cannon tubes. *Materials Evaluation* 39(9): 939-942.

20. Schmitz, V. U., and Becker, F. L. 1982. Scattering of shear wave pulses by surface breaking cracks – time and frequency domain analysis. *Materials Evaluation* 40(2): 191-197.

21. Lott, L. A. 1984 (March). Ultrasonic detection of the molten/solid interfaces of weld pools. *Materials Evaluation* 42.